

# Early Stages of the GRB Explosion

A. M. Beloborodov

*Physics Department, Columbia University, 538 West 120th Street New York, NY 10027*

**Abstract.** Physics of GRB blast waves is discussed with a focus on two effects: (1) pair creation in the external medium by the gamma-ray front and (2) decay of neutrons ahead of the decelerating blast wave. Both effects impact the afterglow mechanism at radii up to  $10^{17}$  cm.

## INTRODUCTION

GRB afterglow is well explained as emission from a decelerating relativistic blast wave. Most of the afterglow data collected to date are obtained relatively late, hours or days after the prompt GRB, when the blast wave is already at final stages of deceleration. *Swift* satellite will provide the missing data on the early stage when the afterglow is most luminous.

The blast wave deceleration begins at a radius  $R_{\text{dec}} \sim 10^{15} - 10^{17}$  cm, which depends on the ambient density  $n_0$  and the initial Lorentz factor  $\Gamma_0$  of the blast wave.<sup>1</sup>  $R_{\text{dec}}$  does not exceed  $10^{17}$  cm, the estimated fireball size during the late afterglow, and can be one or two orders smaller than  $10^{17}$  cm, especially if the circumburst medium has  $R^{-2}$  density profile. Three effects are predicted to occur at  $R \sim 10^{16}$  cm:

- The reverse shock crosses the ejecta and can produce a detectable flash of soft emission (if the ejecta are not dominated by the Poynting flux) [1, 2].
- The external medium ahead of the forward shock is loaded with a large number of  $e^\pm$  pairs by the prompt  $\gamma$ -ray front [3, 4, 5]. The leptonic component of the preshock medium is enriched by  $e^\pm$ , which leads to a dramatic softening of the early afterglow.
- The neutron component of the GRB ejecta overtakes the decelerating blast wave and deposits energy and momentum into the external medium by  $\beta$ -decay [6]. The leading neutron front leaves behind a relativistic trail — a hot mixture of the decay products and ambient particles. The forward shock of the blast wave propagates in this trail instead of the customary ambient medium. The impact of neutrons lasts about 10 e-foldings of the  $\beta$ -decay, and at  $R_{\text{trail}} \approx 10^{17}$  cm the trail becomes static and cold, i.e. indistinguishable from a normal ambient medium.

The paradox of relativistic explosions is that even a small fraction of their energy deposited by a precursor into the external medium impacts the ensuing blast wave and

---

<sup>1</sup>  $\Gamma_0$  can be smaller than the ejecta Lorentz factor  $\Gamma_{\text{ej}}$  if the reverse shock in the ejecta is relativistic, which is the case for a dense external medium.

the afterglow radiation. The importance of both  $\gamma$ -ray and neutron precursors is entirely due to the high Lorentz factor of the explosion. The study of both precursors together is a complicated physical problem and we discuss them separately here.

## ELECTRON-POSITRON LOADING

A medium overtaken by a front of collimated  $\gamma$ -rays is inevitably  $e^\pm$ -loaded [3, 4, 5]. This happens because some  $\gamma$ -rays Compton scatter off the medium and get absorbed by the primary collimated radiation via reaction  $\gamma + \gamma \rightarrow e^+ + e^-$ . The medium is optically thin, so only a tiny fraction of the prompt GRB scatters, however, the number of scattered  $\gamma$ -rays and created  $e^\pm$  *per ambient electron* is huge,  $n_\pm/n_0 \gg 1$ .

The pair loading factor  $Z = 1 + n_\pm/n_0$  does not depend on the ambient density and can be calculated starting with just one ambient electron. The number of  $\gamma$ -rays scattered by the electron at a radius  $R$  is proportional to the column density of the  $\gamma$ -ray front at this radius,  $E_\gamma/4\pi R^2 \propto R^{-2}$ , and therefore  $Z$  is high at small  $R$ .  $Z(R)$  is determined by the isotropic equivalent of the prompt GRB energy  $E_\gamma$  (and slightly depends on the exact spectral shape of the prompt GRB). For the brightest bursts  $E_\gamma > 10^{54}$  erg, and a typical  $E_\gamma \sim 10^{53}$  erg.

The created  $e^\pm$  also scatter radiation, which can lead to an exponential runaway of pair creation. This runaway takes place at radii

$$R < R_{\text{load}} \approx 2 \times 10^{16} (E_\gamma/10^{53})^{1/2} \text{ cm}, \quad (1)$$

leading to  $Z \gg 1$  [5]. The calculation shows also that at  $R < R_{\text{acc}} = R_{\text{load}}/2.3$  the  $e^\pm$ -loaded medium is pushed to relativistic velocities  $\beta\gamma > 1$  by the  $\gamma$ -ray front. The scattered fraction  $\delta E_\gamma$  of the GRB radiation is proportional to the optical depth of the swept-up ambient mass  $m$ , which is proportional to  $n_0$ . However, the medium acceleration  $\gamma = \delta E_\gamma/mc^2$  does not depend on  $n_0$  ( $m$  cancels out), so only  $E_\gamma$  determines  $R_{\text{acc}}$ .

The pair-loading factor  $Z(R)$  and the Lorentz factor  $\gamma(R)$  of a medium overtaken by the GRB radiation front are shown in Fig. 1. These parameters were calculated numerically and approximated by analytical formulae in [5].  $Z$  varies exponentially between  $R_{\text{acc}}$  and  $R_{\text{load}} = 2.3R_{\text{acc}}$  and  $Z(R_{\text{acc}}) \approx 74$ . At  $R < R_{\text{acc}}$  both  $\gamma$  and  $Z$  vary as power-laws with radius. An interesting phenomenon takes place at small radii  $R < R_{\text{gap}} \approx R_{\text{acc}}/3$ : here the external shock may not exist at all because the medium gains so high  $\gamma$  that it runs away from the ejecta and a gap is opened.

The main observational effect of  $e^\pm$ -loading is a strong softening of synchrotron emission from the forward shock. Indeed, the shock energy per proton,  $\Gamma m_p c^2$ , can now be shared by  $Z$  leptons, and the energy per lepton is reduced by the factor  $Z^{-1} \ll 1$ . Then the frequency of synchrotron radiation  $\nu_s$  is reduced as  $Z^{-2}$ . Accurate calculation shows that the preacceleration  $\gamma$  also softens the emission because it reduces the pressure in the blast wave; as a result  $\nu_s \propto Z^{-2} \gamma^{-5/2}$ . This has a strong effect on the early afterglow: it starts as a very soft signal and later evolves to the normal X-ray emission.

The energy dissipated in the forward shock at  $R < R_{\text{load}}$  depends on  $R_{\text{dec}}/R_{\text{load}}$  and can vary. For example, in a medium with  $n_0 \sim 1 - 10 \text{ cm}^{-3}$  (standard ISM) it can be estimated as  $E_{\text{soft}} \approx E(R_{\text{load}}/R_{\text{dec}})^3 = (10^{-3} - 10^{-1})E$  where  $E$  is the ejecta energy

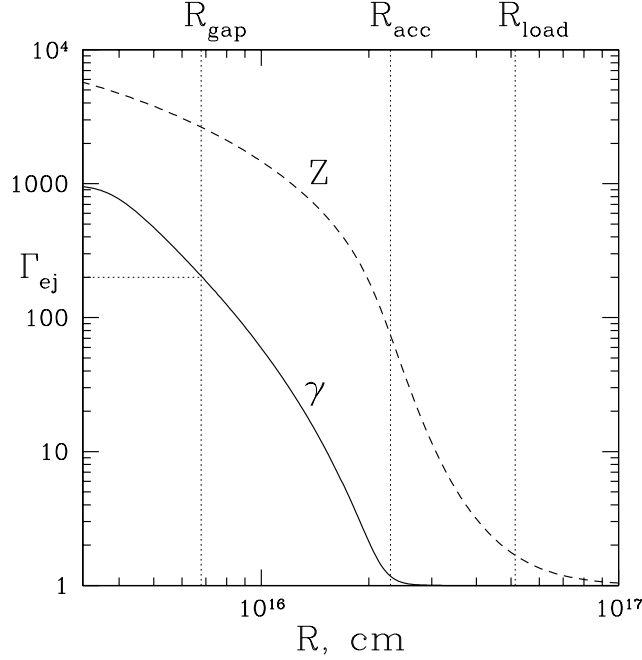


**FIGURE 1.** Pair-loading factor  $Z = 1 + n_{\pm}/n_0$  and acceleration  $\gamma$  of the external medium by the  $\gamma$ -ray front. As the front propagates to larger radii  $R$ , the  $e^{\pm}$  loading and acceleration effects are reduced and become negligible at  $R \approx 10^{17}$  cm. The figure shows the results for GRBs with isotropic energy  $E_{\gamma} = 10^{54}$  erg. The corresponding curves for different  $E_{\gamma}$  are obtained by re-scaling radius  $R \rightarrow R(E_{\gamma}/10^{54})^{1/2}$ . Example ejecta Lorentz factor  $\Gamma_{\text{ej}} = 200$  is indicated;  $\gamma = \Gamma_{\text{ej}}$  defines the gap radius  $R_{\text{gap}}$ .

[5, 7]. The initial soft flash rises sharply at the observer time  $t_{\text{obs}} \sim R_{\text{acc}}/\Gamma_{\text{ej}}^2 c$ , which is before 10 s in most cases, so the rise may be difficult to catch with the current instruments. However, the emission can last much longer after the rise, more than one minute, and then would be easily observed by *Swift*. Estimates of the expected emission have been done in [5, 8, 9], however, the problem requires a more accurate calculation that keeps track of the evolution of each shell in the blast material.

Blast waves in wind-type media ( $n_0 \propto R^{-2}$ ) have small  $R_{\text{dec}}$  [10, 11, 12], and the neglect of  $e^{\pm}$  loading and preacceleration by  $\gamma$ -rays is inconsistent in this situation. The inclusion of these effects leads to a very powerful prompt soft flash because most of the blast wave energy dissipates at  $R < R_{\text{load}}$  [5]. Its detection would be a clear signature of a massive progenitor. On the other hand, the existing upper limits on the early optical emission in several GRBs exclude high-density winds in these bursts.

Optical flashes are also expected from the reverse shocks in the GRB ejecta [1, 2]. The reverse shock with magnetic field  $B$  comparable to that in the forward shock produces an optical flash like the one observed in GRB 990123 [13]. This can be used to probe the composition of the GRB ejecta as the reverse shock emission is sensitive to  $B$ . A magnetic field near or above equipartition with the fluid pressure is likely to suppress the reverse shock component of the afterglow, and then only the  $e^{\pm}$  emission from the forward shock contributes to the optical flash. The forward-shock component does not depend on the nature of the ejecta and can help to determine the ambient density,

magnetic field, and Lorentz factor of the blast wave.

## NEUTRON DECAY

A significant fraction of baryons in the GRB ejecta are neutrons [14, 15, 16]. They are collisionally coupled to the ions when the fireball is accelerated by radiation pressure and develop a high  $\Gamma_n = 10^2 - 10^3$ . Then the neutrons decouple and coast with  $\Gamma_n = \text{const}$ .

The  $\beta$ -decay depletes exponentially the neutron component outside the mean-decay radius  $R_\beta \approx 10^{16}(\Gamma_n/300)$  cm, which is comparable to the expected radius of the early afterglow. However, the neutrons impact the blast wave at radii significantly larger than  $R_\beta$ , even though their number is exponentially reduced at large radii.

The front of survived neutrons overtakes the decelerating blast wave at some radius  $R_*$  where the blast-wave Lorentz factor  $\Gamma$  decreases below  $\Gamma_n$ . Using the Blandford-McKee solution  $\Gamma^2(R) = (17 - 4k)E/8\pi\rho_0c^2R^3$  for adiabatic blast waves in a medium with density  $\rho_0 \propto R^{-k}$  we have

$$R_*^3 = \frac{(17 - 4k)E}{8\pi\rho_0c^2\Gamma_n^2}. \quad (2)$$

At  $R > R_*$  the  $\beta$ -decay takes place in the external medium *ahead* of the forward shock. The impact of this decay can be understood by comparing the energy of neutrons,  $E_n = X_n E \exp(-R/R_\beta)$  ( $X_n$  is the initial neutron fraction of the explosion) with the ambient mass  $mc^2 = \frac{4\pi}{3-k}R^3\rho_0c^2 = \frac{17-4k}{2(3-k)}(E/\Gamma^2)$  they interact with,

$$\frac{E_n}{mc^2} = \frac{2(3-k)}{17-4k}X_n\Gamma^2 \exp\left(-\frac{R}{R_\beta}\right). \quad (3)$$

Just after  $R_*$  this ratio can be as large as  $\Gamma_n^2$  depending on  $R_*/R_\beta$ . The decaying neutron front with  $E_n > mc^2$  deposits huge momentum and energy into the ambient medium, leaving behind a relativistic trail. The exact parameters of this trail are found from energy and momentum conservation applied to the collision of  $\beta$ -decay products with the ambient medium [6].

The ratio  $E_n/mc^2$  becomes smaller than unity only after  $\approx 10$  e-foldings of  $\beta$ -decay. Therefore, the impact of neutrons lasts until  $R_{\text{trail}} \approx 10R_\beta \approx 10^{17}$  cm, and one expects an observational effect if  $R_* < R_{\text{trail}}$ . For a homogeneous medium ( $k = 0$ ) this requires  $n_0 > 0.1E_{52}(\Gamma_n/300)^{-5} \text{ cm}^{-3}$ . For a wind medium ( $k = 2$ )  $R_* < R_{\text{trail}}$  for all plausible parameters of the wind if  $\Gamma_n \sim 10^2$  or higher. Besides, the forward shock in a dense wind is likely to be slow from the very beginning (the reverse shock in the ejecta is relativistic). Then the neutrons can overtake the forward shock immediately, before the self-similar deceleration sets in.

The  $\beta$ -decay ahead of the shock transforms the cold static external medium into a hot, dense, relativistically moving, and possibly magnetized, material. The ion ejecta follow the neutron front and drive a shock wave in the trail material. Dynamics and dissipation in the shock are discussed in [6]. Like the neutron-free shocks, it is difficult to calculate

the expected synchrotron emission from first principles because the electron acceleration and magnetic field evolution are poorly understood. One can apply a phenomenological shock model with the customary parameters  $\epsilon_e$  and  $\epsilon_B$  and fit the data with the model. This may enable an observational test for the  $\beta$ -decay.

Any neutron signature revealed in a GRB afterglow emission would confirm that the ejected baryonic material has gone through a hot high-density phase in the central engine. Neutrons thus provide a unique link between the physics of the central engine and the observed afterglow. Numerical simulations of neutron-fed blast waves may help to identify such signatures. One possibility, for instance, is an exponentially decaying emission component. Another possible signature is a spectral transition or a bump in the afterglow light curve at  $R \approx R_{\text{trail}}$  [6].

Absence of neutron signatures would indicate that the GRB ejecta are dominated by magnetic fields. In such a low-density fireball, the neutrons would decouple early with a modest Lorentz factor and decay quickly. Two-component ejecta with less collimated and less energetic neutrons is possible in the MHD acceleration scenario [17].

## ACKNOWLEDGMENTS

This research was supported by NASA grant NAG5-13382.

## REFERENCES

1. Mészáros, P., & Rees, M. J., ApJ **418**, L59 (1993).
2. Sari, R., & Piran, T. 1999, ApJ, 517, L109 (1999).
3. Thompson, C., & Madau, P., ApJ **538**, 105 (2000).
4. Mészáros, P., Ramirez-Ruiz, E., & Rees, M. J., ApJ **554**, 660 (2001).
5. Beloborodov, A. M., ApJ **565**, 808 (2002).
6. Beloborodov, A. M., ApJL **58**, L19 (2003).
7. Beloborodov, A. M., in "Beaming and Jets in Gamma-Ray Bursts""The Gamma-Ray Universe", astro-ph/0305118 (2003).
8. Li, Z., Dai, Z. G., & Lu, T., MNRAS, in press, astro-ph/0307388 (2003).
9. Kumar, P., & Panaitescu, A., MNRAS, submitted, astro-ph/0309161 (2003).
10. Li, Z.-Y., & Chevalier, R. A., ApJ **589**, L69 (2003).
11. Kobayashi, S., & Zhang, B., ApJ **597**, 459 (2003).
12. Wu, X. F., Dai, Z. G., Huang, Y. F., & Lu, T., MNRAS **342**, 1131 (2003).
13. Akerlof, C. et al., Nature **398**, 400 (1999).
14. Derishev, E. V., Kocharovsky, V. V., & Kocharovsky, V. V., ApJ **521**, 640 (1999).
15. Pruet, J., Woosley, S. E., & Hoffman, R. D., ApJ **586**, 1254 (2003).
16. Beloborodov, A. M., ApJ **588**, 931 (2003).
17. Vlahakis, N., Peng, F., & Königl, A., ApJ **594**, L23 (2003).